

## First Penning trap mass measurement of $^{36}\text{Ca}$

J. Surbrook<sup>1,2</sup>, G. Bollen<sup>1,3</sup>, M. Brodeur<sup>4</sup>, A. Hamaker<sup>1,2</sup>, D. Pérez-Loureiro<sup>2</sup>, D. Puentes<sup>1,2</sup>, C. Nicoloff<sup>1,2</sup>, M. Redshaw<sup>5,2</sup>, R. Ringle<sup>2</sup>, S. Schwarz<sup>2</sup>, C. S. Sumithrarachchi<sup>2</sup>, L. J. Sun<sup>2</sup>, A. A. Valverde<sup>6</sup>, A. C. C. Villari<sup>3</sup>, C. Wrede<sup>1,2</sup> and I. T. Yandow<sup>1,2</sup>

<sup>1</sup>*Department of Physics and Astronomy, Michigan State University, East Lansing, Michigan 48824, USA*

<sup>2</sup>*National Superconducting Cyclotron Laboratory, East Lansing, Michigan 48824, USA*

<sup>3</sup>*Facility for Rare Isotope Beams, East Lansing, Michigan 48824, USA*

<sup>4</sup>*Department of Physics, University of Notre Dame, Notre Dame, Indiana 46556, USA*

<sup>5</sup>*Department of Physics, Central Michigan University, Mount Pleasant, Michigan 48859, USA*

<sup>6</sup>*Department of Physics and Astronomy, University of Manitoba, Winnipeg, Manitoba R3T 2N2, Canada*



(Received 11 May 2020; accepted 7 December 2020; published 29 January 2021)

**Background:** Isobaric quintets provide the best test of the isobaric multiplet mass equation (IMME) and can uniquely identify higher order corrections suggestive of isospin symmetry breaking effects in the nuclear Hamiltonian. The generalized IMME (GIMME) is a novel microscopic interaction theory that predicts an extension to the quadratic form of the IMME. Only the  $A = 20, 32$   $T = 2$  quintets have the exotic  $T_z = -2$  member ground state mass determined to high precision by Penning trap mass spectrometry.

**Purpose:** We aim to establish  $A = 36$  as the third  $T = 2$  isobaric quintet with the  $T_z = -2$  member ground state mass measured by Penning trap mass spectrometry and provide the first test of the predictive power of the GIMME.

**Method:** A radioactive beam of neutron-deficient  $^{36}\text{Ca}$  was produced by projectile fragmentation at the National Superconducting Cyclotron Laboratory. The beam was thermalized and the masses of  $^{36}\text{Ca}^+$  and  $^{36}\text{Ca}^{2+}$  were measured by the time-of-flight ion cyclotron resonance method in the LEBIT 9.4 T Penning trap.

**Results:** We measure the mass excess of  $^{36}\text{Ca}$  to be  $\text{ME} = -6483.6(56)$  keV, an improvement in precision by a factor of 6 over the literature value. The new datum is considered together with evaluated nuclear data on the  $A = 36, T = 2$  quintet. We find agreement with the quadratic form of the IMME given by isospin symmetry, but only coarse qualitative agreement with predictions of the GIMME.

**Conclusion:** A total of three isobaric quintets have their most exotic members measured by Penning trap mass spectrometry. The GIMME predictions in the  $T = 2$  quintet appear to break down for  $A = 32$  and greater.

DOI: [10.1103/PhysRevC.103.014323](https://doi.org/10.1103/PhysRevC.103.014323)

### I. INTRODUCTION

The concept of isospin symmetry, put forth by Heisenberg, is a generalization of the similarities of the proton and neutron under the influence of the strong nuclear force [1]. It treats the proton and neutron as degenerate states of the same hadronic particle and frames an elegant explanation of the similarity of  $p$  and  $n$  masses,  $np$  and  $pp$  nuclear scattering, and properties of atomic nuclei with the same number of total nucleons,  $A$ . Isospin introduces new quantum numbers  $T$  and  $T_z$ . By convention,  $T_z = 1/2$  for the free neutron and  $T_z = -1/2$  for the free proton. In atomic nuclei with  $N$  neutrons and  $Z$  protons, isospin coupling yields  $T_z = (N - Z)/2$  and allows  $T = |T_z|, |T_z| + 1, \dots, A/2$ . Across isobars, states with similar properties can belong to isospin-degenerate multiplets and are called *isobaric analog states* (IAS).

Under isospin symmetry, all members of a multiplet would have the same mass. This symmetry is broken by the mass difference between protons and neutrons and Coulomb interactions between nucleons. First-order perturbation theory

gives a correction to the nuclear mass excess, the *isobaric multiplet mass equation* (IMME) [2]:

$$\text{ME}(A, T, T_z) = a(A, T) + b(A, T)T_z + c(A, T)T_z^2.$$

Coefficients are determined by either theoretical prediction or fitting to measured nuclear masses. Second-order Coulomb effects, three-body interactions, and isospin mixing naturally extend the IMME by adding  $dT_z^3$  and  $eT_z^4$  terms, but the coefficients of these terms have generally been expected to be small ( $\lesssim 1$  keV) [3–5]. Therefore, a need for large  $d$  or  $e$  coefficients to describe a multiplet suggests a breakdown of isospin symmetry. Recent work done with *ab initio* methods (AV18 and AV14 interactions [6] solved with the Brueckner theory [7]) introduce the *generalized IMME* (GIMME) that predicts  $d$  coefficients of a few keV (and smaller  $e$  coefficients) that vary over atomic number  $A$ . These nonzero coefficients arise from the density dependence of isospin non-conserving effects in the nuclear medium and Coulomb

polarization effects in the common proton-neutron “core” of a multiplet [8,9].

Higher-order coefficients in the IMME are best searched for in  $T = 2$  quintets, where  $d$  and  $e$  coefficients can be uniquely determined simultaneously. Often, the largest challenge in measurement of a quintet’s IMME coefficients is the difficulty of precision measurement of the neutron-deficient  $T_z = -2$  member. The short half-lives and challenging production, due to proximity to the proton drip line, of these members limit the range of experimental measurement techniques capable of keV-level precision. As such, only two quintets exist ( $A = 20, 32$ ) [10–12] with all members’ ground state masses measured to keV-level precision. In both cases,  $^{20}\text{Mg}$  ( $A = 20, T_z = -2$ ) and  $^{32}\text{Ar}$  ( $A = 32, T_z = -2$ ) were measured by Penning trap mass spectrometry, the most precise method of determining atomic mass [11,13,14]. The current mass excess of  $^{36}\text{Ca}$ ,  $\text{ME} = -6450(40)$  keV, has remained unchallenged since the measurement of the  $^{40}\text{Ca}(^4\text{He}, ^8\text{He})^{36}\text{Ca}$  neutron-knockout reaction  $Q$  value was published in 1977 [11,15]. Another reaction measurement around 1998 remains unpublished [16–18]. A Penning trap mass measurement of  $^{36}\text{Ca}$  would mark the third (and heaviest) IMME quintet with the challenging  $T_z = -2$  member measured to high precision by Penning trap mass spectrometry. The complementary  $A = 36$  members are already known to a satisfactory precision through a combination of mass measurements involving Penning traps and careful particle threshold measurements [11]. Additionally, the GIMME predicts the  $A = 36$  quintet  $d$  coefficient to have the largest departure from the quadratic IMME, making the mass measurement of  $^{36}\text{Ca}$  particularly relevant [9].

## II. EXPERIMENT

At the National Superconducting Cyclotron Laboratory (NSCL), a primary beam of  $^{40}\text{Ca}$  was accelerated to 140 MeV/nucleon with the Coupled Cyclotron Facility and impinged on a 658 mg/cm<sup>2</sup> thick target of beryllium to produce  $^{36}\text{Ca}^{20+}$  ( $t_{1/2} = 102(2)$  ms [19]). The cocktail secondary beam was transported to the A1900 fragment separator [20], where magnetic isotopic-selection transported a purified ( $\approx 1\%$ ) beam of  $^{36}\text{Ca}^{20+}$  to the NSCL gas cell [21]. Aluminum degraders and high-purity helium gas in the gas cell (95 mbar) stopped the fast beam. Internal radio frequency quadrupole electrodes guided ions out of the gas cell volume to vacuum, where a dipole magnet of resolving power  $\approx 1500$  selected ions of a specific mass-to-charge ratio  $A/Q$ . Ions were transported to the Low-Energy Beam and Ion Trap (LEBIT) facility, which is unparalleled among Penning trap facilities for its ability to measure the mass of short-lived rare isotopes produced by projectile fragmentation [22]. Figure 1 shows a schematic of the gas cell and LEBIT facility.

In LEBIT, the masses of  $^{36}\text{Ca}^+$  and  $^{36}\text{Ca}^{2+}$  were measured by the time-of-flight ion cyclotron resonance method [23]. Following production, the ion beam is stopped, cooled, and accumulated to form ion bunches in low-pressure helium gas ( $3 \times 10^{-2}$  mbar cooling,  $5 \times 10^{-4}$  mbar bunching) [24]. After an accumulation time of 100–200 ms, a short  $< 10$   $\mu\text{s}$  bunch is ejected. A fast electrostatic kicker provides additional  $A/Q$  se-

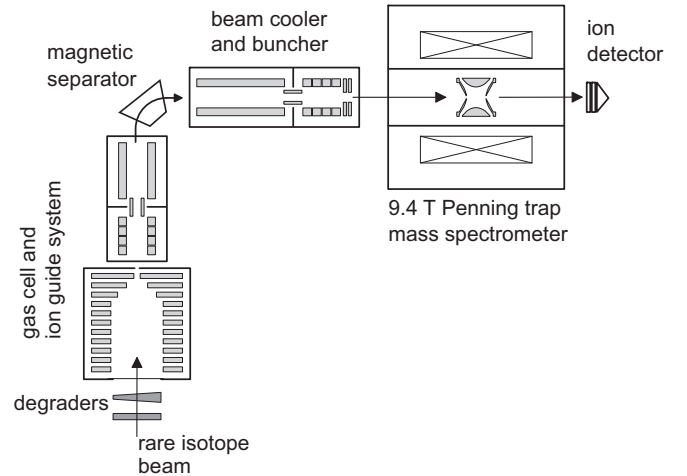


FIG. 1. Schematic of the NSCL gas cell and LEBIT facility. For further discussion, see Ref. [22].

lection by time-of-flight (TOF) filtering before the ion bunch passes into the LEBIT Penning trap, a high-precision hyperbolic electrode trap system housed in a 9.4 T superconducting solenoidal magnet [25]. In the trap, the ion’s motion is described by three eigenmotions with characteristic frequencies ( $\nu_i$ ): trap axial ( $\nu_z$ ), magnetron ( $\nu_-$ ), and modified cyclotron ( $\nu_+$ ), as described in Ref. [26]. The ion bunch is purified by simultaneously applying a sum of dipole radio frequency electric field (RF) at the modified-cyclotron frequencies of identified contaminant ions and the stored waveform inverse Fourier transform (SWIFT) technique, a dipole RF excitation waveform calculated to emulate a fixed-period 10 kHz RF window outside  $\nu_+$  of the ion of interest [27,28]. This dipole RF excites contaminant ions’ modified-cyclotron motion out of the trap sensitive volume, reducing the measurement of trapped contaminant ions. Quadrupolar RF with a frequency  $\nu_{RF}$  is applied in the trap near cyclotron frequency  $\nu_c = \nu_- + \nu_+$  of the ion of interest to convert initial magnetron motion created by Lorentz steerers [25] to modified-cyclotron motion. Ions are ejected to a multichannel plate detector outside of the 9.4 T magnet, where the ions’ time of flight is measured. This procedure is repeated while scanning  $\nu_{RF}$  near  $\nu_c$  to create a TOF curve as in Fig. 2. The ion’s TOF is minimized for  $\nu_{RF} = \nu_c$ .

The measurement was performed across two settings after a search for  $\beta$  radioactivity in a silicon detector, located after the gas cell dipole magnet, for a variety of  $A/Q$  settings. We first set the gas cell dipole magnet to select  $A/Q = 36$  and measured the cyclotron frequency of  $^{36}\text{Ca}^+$  in the Penning trap. The reference measurement for this setting was  $^{12}\text{C}_3^+$  (Setting I). We then set the gas cell dipole magnet for  $A/Q = 45$ , selecting for molecular  $^{36}\text{Ca}(\text{H}_2\text{O})_3^{2+}$ . A potential difference of 100 V was applied between the gas cell and the LEBIT cooler and buncher to liberate  $^{36}\text{Ca}^{2+}$  via collision-induced disassociation [29]. The cyclotron frequency of  $^{36}\text{Ca}^{2+}$  was measured in the Penning trap, using  $\text{H}_2\text{O}^+$  as the reference (Setting II). Both settings excited the  $^{36}\text{Ca}$  ions for 50 ms per scan to limit losses of  $^{36}\text{Ca}$  ions due to decay. Frequency measurements of the ion of interest and the reference ion were

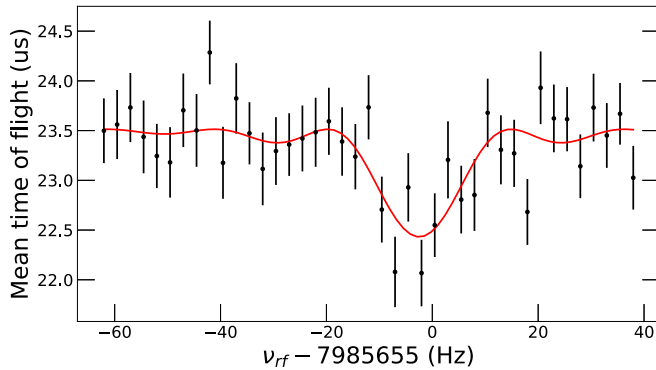


FIG. 2. Time-of-flight resonance of  $^{36}\text{Ca}^{2+}$  with 50 ms excitation time. The smooth curve shows the fit of the theoretical curve used to extract  $\nu_c$  [30].

alternated in time, with no measurement running longer than 90 minutes.

### III. ANALYSIS

We determine the mass of the ion of interest by calculating the ratio of the ion-of-interest (ion) cyclotron frequency and the interpolated cyclotron frequency of the reference ion (ref),  $R = \nu_{\text{ref}}/\nu_{\text{ion}}$ . Figure 2 shows one time-of-flight spectrum used to extract a cyclotron frequency of  $^{36}\text{Ca}^{2+}$ . The analytic form of the TOF response curve of an ion excited in the Penning trap is presented in Ref. [30]. The full shape of the TOF curve was fit to data by  $\chi^2$  minimization and the cyclotron frequency was extracted. The mass of the ion of interest is then  $M = (q/q_{\text{ref}})R(m_{\text{ref}} - q_{\text{ref}}m_e) + qm_e$ . For Setting I,  $q = 1$  and for Setting II,  $q = 2$ . The reference ion was singly charged in both settings, so  $q_{\text{ref}} = 1$ . We measured  $R = 1.000\,193\,69(50)$  for Setting I and  $R = 1.000\,780\,41(18)$  for Setting II. Mass-dependent systematic shifts, such as those due to inhomogeneities in the magnetic field or imperfections in the trap geometry, have been investigated at LEBIT and characterized at  $\Delta R \approx 2 \times 10^{-10}/u$  [31]. The use of  $A/Q = 36$  and 18 mass doublets, for Settings I and II respectively, renders such mass-dependent systematics negligible. Effects due to special relativity are estimated to  $\Delta R \leq 10^{-11}$ . Nonlinear fluctuations in the magnetic field have been shown to yield  $\Delta R < 10^{-9}/\text{hour}$  [32]. Shifts due to ion-ion interactions are below our statistical uncertainty: more than 75% of nonempty bunches contained a single ion and bunches with 5 or more ions were discarded from the analysis. Varying this maximum ion-count cutoff from 1 to 5 ions yields  $\Delta R \approx 10^{-8}$ . As these systematic effects are well controlled relative to our statistical precision ( $\approx 10^{-7}$ ), they were considered to be negligible in the analysis. While each setting has a limited number of measurements, the near-unity Birge ratio [33] [Setting I: 0.56(33); Setting II: 0.81(27)] of each setting suggests that the assigned statistical error bars are appropriate. We used the most recent Atomic Mass Evaluation [11] for the mass of the reference ion in each setting to calculate the mass excess of  $^{36}\text{Ca}$ . The chemical binding energy ( $\approx 10$  eV) was treated as negligible. The two settings yield  $\text{ME}_{\text{setting-I}} = -6494(17)$  keV and  $\text{ME}_{\text{setting-II}} = -6482.3(59)$  keV, for an error-weighted aver-

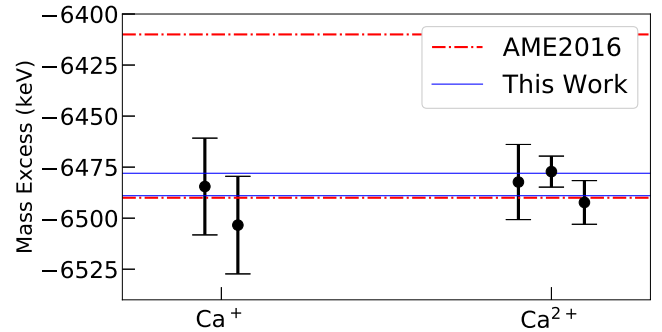


FIG. 3. Mass excess of  $^{36}\text{Ca}$  determined by measurements of  $^{36}\text{Ca}^+$  and  $^{36}\text{Ca}^{2+}$  and their  $1\sigma$  error bars. The horizontal lines show the  $1\sigma$  error band from the AME2016 (dot-dashed red) [11,15] and this work (solid blue). Note the near overlap of lower-bound lines near  $\text{ME} \approx -6490$  keV.

aged value of  $\text{ME} = -6483.6(56)$  keV, shown in Fig. 3. The agreement between the two  $A/Q$  settings demonstrates the strong constraints on  $A/Q$ -dependent systematic effects.

### IV. DISCUSSION

A literature search for updates to the  $A = 36$  quintet found the most recent IMME [10] and atomic mass [11] evaluations to be current. We adopted these values, replacing the previous  $^{36}\text{Ca}$  measurement by our new value with 6 times more precision, and performed quadratic, cubic, quadratic +  $eT_z^4$ , and quartic fits by  $\chi^2$  minimization to extract coefficients of the extended IMME. Table I gives the inputs for this analysis and Table II presents the output coefficients. We find that the quadratic model describes the  $A = 36$ ,  $T = 2$  quintet well, with a chi-square per degree of freedom of  $\chi^2/\nu = 0.65/2$  ( $p$  value of 0.72). Furthermore, the quartic fit yields  $d = -0.4(6)$  keV and  $e = 0.2(6)$  keV, both of which are consistent with the IMME prediction of zero.  $A = 36$  now has the second most precise measurement of  $T = 2$  IMME coefficients, following  $A = 32$ .

#### A. The GIMME

We plot the  $T = 2$  IMME  $d$  and  $e$  coefficients in Fig. 4, similar to the presentation in Ref. [9], updated with the present work on the  $A = 36$  quintet. Our new calculation of the

TABLE I. Mass excesses (ME) and excitation energy of the isobaric analog states ( $E_{\text{IAS}}$ ) used to tabulate the mass excess of IAS states ( $\text{ME}_{\text{IAS}}$ ) in our analysis. The  $^{36}\text{Ca}$  value is from the present measurement. Previous values are incorporated from Refs. [10,11].

| Species          | ME (keV)         | $E_{\text{IAS}}$ (keV) | $\text{ME}_{\text{IAS}}$ (keV) |
|------------------|------------------|------------------------|--------------------------------|
| $^{36}\text{Ca}$ | $-6483.6(56)$    |                        | $-6483.6(56)$                  |
| $^{36}\text{K}$  | $-17417.1(3)$    | 4282.4(24)             | $-13134.6(24)$                 |
| $^{36}\text{Ar}$ | $-30231.540(27)$ | 10852.1(12)            | $-19379.4(12)$                 |
| $^{36}\text{Cl}$ | $-29522.01(4)$   | 4299.667(14)           | $-25222.35(4)$                 |
| $^{36}\text{S}$  | $-30664.12(19)$  |                        | $-30664.12(19)$                |

TABLE II. Updated coefficients of several variations of the IMME and the quality of fit, described by chi-squared per degree of freedom and corresponding  $p$  value. Experimental inputs are given in Table I.

| $a$                | $b$               | $c$             | $d$            | $e$            | $\chi^2/\nu$ | $p$ value |
|--------------------|-------------------|-----------------|----------------|----------------|--------------|-----------|
| $-19378.9 \pm 0.5$ | $-6044.2 \pm 0.8$ | $200.8 \pm 0.3$ |                |                | 0.646/2      | 0.724     |
| $-19379.6 \pm 1.0$ | $-6043.8 \pm 1.0$ | $201.3 \pm 0.7$ | $-0.3 \pm 0.4$ |                | 0.077/1      | 0.781     |
| $-19379.4 \pm 1.2$ | $-6044.4 \pm 0.9$ | $201.6 \pm 1.8$ |                | $-0.1 \pm 0.3$ | 0.463/1      | 0.496     |
| $-19379.4 \pm 1.2$ | $-6043.5 \pm 1.7$ | $200.8 \pm 2.2$ | $-0.4 \pm 0.6$ | $0.2 \pm 0.6$  |              |           |

experimental  $d$  coefficient is consistent with the IMME ( $\delta \approx 0.7\sigma$ ) and less so with the GIMME prediction ( $d_{\text{GIMME}} = -1.98$ ,  $\delta \approx 2.6\sigma$ ), where  $\delta$  is the prediction/experiment difference and  $\sigma$  is the one-standard-deviation experimental error. The experimental  $d$  coefficient is between the predictions of the IMME and GIMME, as in the  $A = 20, 24$  quintets. The  $e$  coefficient is consistent with both the IMME and GIMME ( $e_{\text{GIMME}} = 0.114$ ), but the predictions of the GIMME are small across  $A$  and, therefore, similar to the IMME.

Currently, no experimental  $e$  coefficient can discriminate between the two predictions, as their difference is beyond an order of magnitude smaller than most of the quintets' experimental error bars. The oscillatory behavior of the  $d$  coefficient over  $A$  predicted by the GIMME (and strongly evidenced in the  $T = 3/2$  quartets) appears muted in the  $T = 2$  cases. The oscillatory pattern in the GIMME theory papers [8,9] was attributed to nuclear shell structure, with predictions of small  $d$ ,  $e$  coefficients in multiplets containing magic or near-magic numbers, so it is peculiar to see only weak experimental evidence in  $T = 2$ .

We do not rule out the GIMME prediction for  $A = 36$ . This rough compatibility highlights the nearby  $A = 32$  quintet, which departs from both the IMME and GIMME with a positive  $d$  coefficient,  $d_{\text{exp}} = 0.90(19)$  keV [10]. A recent theoretical discussion of the  $A = 32$  quintet [34] framed this departure from the quadratic IMME as a consequence of isospin mixing. Isospin mixing strength was calculated with the USD, USDA, USDB shell model interactions and each

predicted a positive  $d$  coefficient ( $d_{\text{theory}} = 0.28\text{--}0.39$  keV), similar to, but smaller than, the experimental value. However, mixing strength depends strongly on the precise difference in energy of nearby states capable of mixing with the IAS. A confounding factor of these calculations is the 100–150 keV rms deviation typical of the empirical interactions; a 100 keV shift in any of the participating states' energy lends itself to a considerable change in the shift of the IAS predicted due to isospin mixing. The work predicted nearby ( $\Delta[E_i - E_{\text{IAS}}] < 500$  keV) states in both  $^{32}\text{Cl}$  and  $^{32}\text{S}$  that shift the members' IAS energy by  $>1$  keV (although the  $d$  coefficient is not sensitive to shifts in the  $T_z = 0$ ,  $^{32}\text{S}$ , IAS energy). Experimental spectroscopic data of these levels is insufficient to control for differences of the predicted mixing-states' energies across the utilized interactions. In the  $A = 36$  multiplet, despite strong agreement with the zero  $d$  coefficient of the IMME, a theoretical work similar to Ref. [34] would be useful, along with appropriately detailed spectroscopy, especially in  $^{36}\text{K}$ .

## B. Outlook

Given the agreement between experiment and GIMME prediction for the  $A = 20, 24$  quintets and the tension in the  $A = 32, 36$  quintets, it is important to precisely measure the quintets in the middle. In both the  $A = 24, 28$  quintets, uncertainty contribution in the  $d$  and  $e$  coefficients is led by the ground state mass measurements of the  $T_z = -2$  members, ( $^{24}\text{Si}$ ,  $^{28}\text{S}$ ). The mass of  $^{24}\text{Si}$  was recently measured by LEBIT to a precision that may offer discrimination between the IMME and GIMME predictions, and the publication is currently being prepared. A measurement of  $^{28}\text{S}$  will finish the  $A = 28$  quintet, giving IMME coefficients from  $A = 20\text{--}36$  in regular steps of  $\delta A = 4$ . Additionally, paired with recent proton-separation energy measurements [35], a high-precision measurement of  $^{28}\text{S}$  would update the mass of  $^{29}\text{Cl}$  and may clarify the source of the large  $T = 5/2$ ,  $A = 29$   $d$  coefficient [ $d = 28(7)$  keV], the largest measured cubic coefficient across all masses and isospin [36].

In principle,  $T = 2$  quintets of mass  $A = 40$  and higher may be accessible experimentally. The  $A = 40$  quintet currently would benefit from Penning trap mass measurements of both  $T_z = -1$  ( $^{40}\text{Sc}$ ) and  $T_z = -2$  ( $^{40}\text{Ti}$ ) members. A challenge to these measurements is low production cross-sections due to these isotopes' proximity to the proton drip line. Additionally, the measured half-lives of  $T_z = -2$  members are the shortest of a multiplet's members. Advanced Penning trap techniques like phase-imaging ion cyclotron resonance (PI-ICR) [37–39] will extend the half-life and precision reach

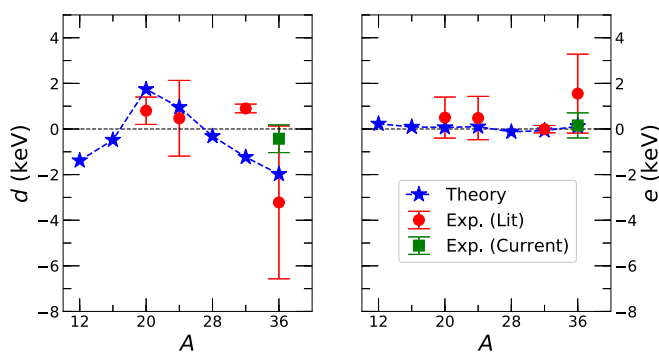


FIG. 4.  $d$  and  $e$  coefficients of the  $T = 2$  quartic IMME. The star points come from GIMME theory [9]. The circular points are from the experimental literature [10,12] and the square point is the update to the  $A = 36$  quintet from this work. Those quintets with experimental error bars larger than the figure are omitted. Update to Fig. 3 from Ref. [9].



of Penning trap mass measurements with rare isotopes, and next-generation fragmentation facilities such as the Facility for Rare Isotope Beams in East Lansing, Michigan, USA are expected to have favorable beam rates. For most  $A = 4n + 2$  quintets ( $n$  is an integer), the  $T_z = -2$  members are proton unbound. The exceptions are  $A = 22, 26$ ; however, no  $T = 2$  IAS have yet been identified in odd-odd  $T_z = 0$  nuclei  $^{22}\text{Na}$  and  $^{26}\text{Al}$ .

Despite this discussion's focus of testing the GIMME  $d$  coefficient predictions, the GIMME predicts nonzero  $e$  coefficients that will be experimentally accessible in the near future. Based on previously achieved precision in the best-measured IAS excitation energies ( $\sigma_{E,\text{IAS}} \lesssim 100$  eV [10]) and the cited PI-ICR measurements with 100–200 ms accumulation times [37,38], it should be a goal to test the GIMME  $e$  coefficients. By setting a precision goal of 100 eV in the ground state mass measurements and the IAS excited state spectroscopy (in tandem with the previously mentioned search for isospin mixing states), one may begin to search for anomalous  $e$  coefficients equal in magnitude to the GIMME predictions at a  $2\sigma$ – $3\sigma$  level ( $|e_{\text{GIMME}}| \approx 0.07$ – $0.11$  keV).

Achieving experimental precision of  $\lesssim 100$  eV across a isospin multiplet would strengthen a suite of experimental tests of the Standard Model that are sensitive to the  $Q$  value of the superallowed beta decay of the  $T_z = -2$  member of a multiplet. The precise measurements of  $T = 2$  superallowed  $0^+ \rightarrow 0^+$  decay properties, such as those measured in the decay of  $^{32}\text{Ar}$  in Ref. [40], become well-positioned to build upon the comprehensive evaluation of  $T = 1$  superallowed  $0^+ \rightarrow 0^+$  decays by Towner and Hardy [41] testing the conserved vector current hypothesis and consequentially providing the most precisely known element in the quark-mixing Cabibbo-Kobayashi-Maskawa matrix. Scalar currents in the weak interaction can be probed by measuring the beta-neutrino angular correlation in the decays of  $T = 2$  nuclei, and modern programs stand to improve on earlier work done with  $^{32}\text{Ar}$  [42] (TAMUTRAP [43,44], WISArD [45,46]). Additionally, one may set limits on electron–sterile-neutrino mixing from precision measurements of the beta-particle

energy distribution [47,48]. Currently, the  $Q$  value of the superallowed beta decay of  $^{32}\text{Ar}$  is the only  $T = 2$  beta-decay energy measurement approaching the precision required for these tests ( $\sigma_Q = 1.9$  keV [10]), and a catalog of precisely measured ( $\sigma_Q \lesssim 100$  eV)  $T = 2$   $Q$  values would afford novel-physics searches a valuable range of nuclei to benchmark nuclear-physics-driven systematic effects.

## V. CONCLUSIONS

We have reported the mass excess of neutron-deficient  $^{36}\text{Ca}$ , measured directly for the first time with the time-of-flight ion cyclotron resonance method in the LEBIT 9.4 T Penning trap at the National Superconducting Cyclotron Laboratory. This completes the third isobaric quintet with the challenging  $T_z = -2$  member ground state mass determined to high-precision with Penning trap mass spectrometry. We interpreted this new result in the context of the isobaric multiplet mass equation and a new *ab initio* derived calculation that naturally extends the IMME. We find excellent agreement in the  $A = 36, T = 2$  isobaric multiplet with the quadratic IMME, and only coarse qualitative agreement with the new GIMME predictions. Tension is emerging between GIMME  $T = 2$  predictions and experimental measurements for  $A = 32$  and heavier.

## ACKNOWLEDGMENTS

We thank J. M. Dong for sharing the numerical predictions from the GIMME theory to make Fig. 4 and Marion MacCormick for discussion on the IMME. This work was conducted with the support of Michigan State University, the National Science Foundation under Contracts No. PHY-1565546, No. PHY-1713857, and No. PHY-1913554, the U.S. Department of Energy, Office of Science, Office of Nuclear Physics under Grants No. DE-SC-0015927 and No. DE-SC-0016052, and Natural Sciences and Engineering Research Council of Canada under Contract No. SAPPJ-2018-00028.

- 
- [1] W. Heisenberg, *Z. Phys.* **77**, 1 (1932).  
 [2] S. Weinberg and S. B. Treiman, *Phys. Rev.* **116**, 465 (1959).  
 [3] E. M. Henley and C. E. Lacy, *Phys. Rev.* **184**, 1228 (1969).  
 [4] J. Jänecke, *Nucl. Phys. A* **128**, 632 (1969).  
 [5] G. Bertsch and S. Kahana, *Phys. Lett. B* **33**, 193 (1970).  
 [6] R. B. Wiringa, V. G. J. Stoks, and R. Schiavilla, *Phys. Rev. C* **51**, 38 (1995).  
 [7] K. Brueckner, J. Gammel, and H. Weitzner, *Phys. Rev.* **110**, 431 (1958).  
 [8] J. M. Dong, Y. H. Zhang, W. Zuo, J. Z. Gu, L. J. Wang, and Y. Sun, *Phys. Rev. C* **97**, 021301(R) (2018).  
 [9] J. M. Dong, J. Z. Gu, Y. H. Zhang, W. Zuo, L. J. Wang, Y. A. Litvinov, and Y. Sun, *Phys. Rev. C* **99**, 014319 (2019).  
 [10] M. MacCormick and G. Audi, *Nucl. Phys. A* **925**, 61 (2014).  
 [11] M. Wang, G. Audi, F. G. Kondev, W. J. Huang, S. Naimi, and X. Xu, *Chin. Phys. C* **41**, 030003 (2017).  
 [12] B. E. Glassman, D. Pérez-Loureiro, C. Wrede, J. Allen, D. W. Bardayan, M. B. Bennett, B. A. Brown, K. A. Chipps, M. Febraro, C. Fry, M. R. Hall, O. Hall, S. N. Liddick, P. O'Malley, W. Ong, S. D. Pain, S. B. Schwartz, P. Shidling, H. Sims, P. Thompson, and H. Zhang, *Phys. Rev. C* **92**, 042501(R) (2015).  
 [13] K. Blaum, *Phys. Rep.* **425**, 1 (2006).  
 [14] D. Lunney, J. M. Pearson, and C. Thibault, *Rev. Mod. Phys.* **75**, 1021 (2003).  
 [15] R. E. Tribble, J. D. Cossairt, and R. A. Kenefick, *Phys. Rev. C* **15**, 2028 (1977).  
 [16] A. Komives, A. García, D. Peterson, D. Bazin, J. Caggiano, B. Sherrill, N. Alahari, A. Bacher, W. Lozowski, J. Greene, and E. G. Adelberger, *APS Division of Nuclear Physics Meeting Abstracts*, APS Meeting Abstracts (NASA, Washington, DC, 1998), p. F3.07.  
 [17] J. Greene, G. Thomas, A. García, A. Komives, and J. O. Stoner, Jr., *Nucl. Instrum. Methods Phys. Res. A* **438**, 52 (1999).  
 [18] J. A. Caggiano, Spectroscopy of exotic nuclei with the S800 spectrograph, Ph.D. thesis, Michigan State University,

- 1999, [https://publications.nsl.msui.edu/thesis/Caggiano\\_1999\\_21.pdf](https://publications.nsl.msui.edu/thesis/Caggiano_1999_21.pdf).
- [19] N. Nica, J. Cameron, and B. Singh, *Nucl. Data Sheets* **113**, 1 (2012).
- [20] D. J. Morrissey, B. M. Sherrill, M. Steiner, A. Stolz, and I. Wiedenhoever, *Nucl. Instrum. Methods Phys. Res. B* **204**, 90 (2003).
- [21] C. S. Sumithrarachchi, D. Morrissey, S. Schwarz, K. Lund, G. Bollen, R. Ringle, G. Savard, and A. C. C. Villari, *Nucl. Instrum. Methods Phys. Res. B* **463**, 305 (2020).
- [22] R. Ringle, S. Schwarz, and G. Bollen, *Int. J. Mass Spectrom.* **349-350**, 87 (2013).
- [23] G. Gräff, H. Kalinowsky, and J. Traut, *Z. Phys. A* **297**, 35 (1980).
- [24] S. Schwarz, G. Bollen, R. Ringle, J. Savory, and P. Schury, *Nucl. Instrum. Methods Phys. Res. A* **816**, 131 (2016).
- [25] R. Ringle, G. Bollen, A. Prinke, J. Savory, P. Schury, S. Schwarz, and T. Sun, *Int. J. Mass Spectrom.* **263**, 38 (2007).
- [26] L. S. Brown and G. Gabrielse, *Phys. Rev. A* **25**, 2423 (1982).
- [27] M. Redshaw, G. Bollen, S. Bustabad, A. A. Kwiatkowski, D. L. Lincoln, S. J. Novario, R. Ringle, S. Schwarz, and A. A. Valverde, *Nucl. Instrum. Methods Phys. Res. B* **317**, 510 (2013).
- [28] A. A. Kwiatkowski, G. Bollen, M. Redshaw, R. Ringle, and S. Schwarz, *Int. J. Mass Spectrom.* **379**, 9 (2015).
- [29] P. Schury, G. Bollen, M. Block, D. J. Morrissey, R. Ringle, A. Prinke, J. Savory, S. Schwarz, and T. Sun, *Hyperfine Interact.* **173**, 165 (2006).
- [30] M. König, G. Bollen, H.-J. Kluge, T. Otto, and J. Szerypo, *Int. J. Mass Spectrom. Ion Proc.* **142**, 95 (1995).
- [31] K. Gulyuz, J. Ariche, G. Bollen, S. Bustabad, M. Eibach, C. Izzo, S. J. Novario, M. Redshaw, R. Ringle, R. Sandler, S. Schwarz, and A. A. Valverde, *Phys. Rev. C* **91**, 055501 (2015).
- [32] R. Ringle, T. Sun, G. Bollen, D. Davies, M. Facina, J. Huikari, E. Kwan, D. J. Morrissey, A. Prinke, J. Savory, P. Schury, S. Schwarz, and C. S. Sumithrarachchi, *Phys. Rev. C* **75**, 055503 (2007).
- [33] R. T. Birge, *Phys. Rev.* **40**, 207 (1932).
- [34] A. Signoracci and B. A. Brown, *Phys. Rev. C* **84**, 031301(R) (2011).
- [35] I. Mukha, L. V. Grigorenko, X. Xu, L. Acosta, E. Casarejos, A. A. Ciemny, W. Dominik, J. Duénas-Díaz, V. Dunin, J. M. Espino, A. Estradé, F. Farinon, A. Fomichev, H. Geissel, T. A. Golubkova, A. Gorshkov, Z. Janas, G. Kamiński, O. Kiselev, R. Knöbel *et al.*, *Phys. Rev. Lett.* **115**, 202501 (2015).
- [36] M. Brodeur, A. A. Kwiatkowski, O. M. Drozdowski, C. Andreoiu, D. Burdette, A. Chaudhuri, U. Chowdhury, A. T. Gallant, A. Grossheim, G. Gwinner, H. Heggen, J. D. Holt, R. Klawitter, J. Lassen, K. G. Leach, A. Lennarz, C. Nicoloff, S. Raeder, B. E. Schultz, S. R. Stroberg, A. Teigelhöfer, R. Thompson, M. Wieser, and J. Dilling, *Phys. Rev. C* **96**, 034316 (2017).
- [37] S. Eliseev, K. Blaum, M. Block, C. Droese, M. Goncharov, E. Minaya Ramirez, D. A. Nesterenko, Y. N. Novikov, and L. Schweikhard, *Phys. Rev. Lett.* **110**, 082501 (2013).
- [38] D. A. Nesterenko, T. Eronen, A. Kankainen, L. Canete, A. Jokinen, I. D. Moore, H. Penttilä, S. Rinta-Antila, A. de Roubin, and M. Vilen, *Eur. Phys. J. A* **54**, 154 (2018).
- [39] R. Orford, J. A. Clark, G. Savard, A. Aprahamian, F. Buchinger, M. T. Burkey, D. A. Gorelov, J. W. Klimes, G. E. Morgan, A. Nystrom, W. S. Porter, D. Ray, and K. S. Sharma, *Nucl. Instrum. Methods Phys. Res. B* **463**, 491 (2020).
- [40] M. Bhattacharya, D. Melconian, A. Komives, S. Triambak, A. García, E. G. Adelberger, B. A. Brown, M. W. Cooper, T. Glasmacher, V. Guimaraes, P. F. Mantica, A. M. Oros-Peusquens, J. I. Prisciandaro, M. Steiner, H. E. Swanson, S. L. Tabor, and M. Wiedeking, *Phys. Rev. C* **77**, 065503 (2008).
- [41] J. C. Hardy and I. S. Towner, *Phys. Rev. C* **91**, 025501 (2015).
- [42] E. G. Adelberger, C. Ortiz, A. García, H. Swanson, M. Beck, O. Tengblad, M. J. G. Borge, I. Martel, H. Bichsel, and the ISOLDE Collaboration, *Phys. Rev. Lett.* **83**, 1299 (1999).
- [43] M. Mehlman, P. D. Shidling, S. Behling, L. G. Clark, B. Fenker, and D. Melconian, *Nucl. Instrum. Methods Phys. Res. A* **712**, 9 (2013).
- [44] P. D. Shidling, V. S. Kolhinen, B. Schroeder, N. Morgan, A. Ozmetin, and D. Melconian, *Hyperfine Interact.* **240**, 40 (2019).
- [45] P. Ascher, B. Blank, M. Gerbaux, J. Giovinazzo, S. Grévy, T. Kurtukian Nieto, N. Severijns, V. Araujo-Escalona, G. Ban, X. Fléchar, E. Liénard, G. Quéméner, and D. Zakoucky, WISARD: Weak-interaction studies with  $^{32}\text{Ar}$  decay, CERN Technical Report CERN-INTC-2016-050, INTC-I-172, 2016, <https://cds.cern.ch/record/2222309>.
- [46] V. Araujo-Escalona, D. Atanasov, X. Fléchar, P. Alfaut, P. Ascher, B. Blank, L. Daudin, M. Gerbaux, J. Giovinazzo, S. Grévy, T. Kurtukian-Nieto, E. Liénard, G. Quéméner, N. Severijns, S. Vanlangendonck, M. Versteegen, and D. Zakoucky, *Phys. Rev. C* **101**, 055501 (2020).
- [47] R. E. Shrock, *Phys. Lett. B* **96**, 159 (1980).
- [48] D. A. Bryman and R. Shrock, *Phys. Rev. D* **100**, 073011 (2019).